Quantum cutting downconversion by cooperative energy transfer from Bi^{3+} to Yb^{3+} in Y_2O_3 phosphor*

Wei Xian-Tao(韦先涛), Zhao Jiang-Bo(赵江波), Chen Yong-Hu(陈永虎), Yin Min(尹 民)†, and Li Yong(李 勇)

Department of Physics, University of Science and Technology of China, Hefei 230026, *China*

(Received 25 June 2009; revised manuscript received 18 September 2009)

Bi^{3+} and Yb^{3+} codoped cubic Y_2O_3 phosphors are prepared by pechini sol–gel method. Strong near-infrared (NIR) emission around 980 nm from Yb^{3+} ($^2F_{5/2} \rightarrow ^2F_{7/2}$) is observed under ultraviolet light excitation. A broad excitation band ranging from 320 to 360 nm, owing to the $6s^2 \rightarrow 6s6p$ transition of Bi^{3+} ions, is recorded when the Yb^{3+} emission is monitored, which suggests a very efficient energy transfer from Bi^{3+} ions to Yb^{3+} ions. The Yb^{3+} concentration dependences of both the Bi^{3+} and the Yb^{3+} emissions are investigated. The decay curve of Bi^{3+} emission under the excitation of 355 nm pulse laser is used to explore the $Bi^{3+} \rightarrow Yb^{3+}$ energy transfer process. Cooperative energy transfer (CET) is discussed as a possible mechanism for the near-infrared emission.

Keywords: downconversion, cooperative energy transfer, photoluminescence
PACC: 7855, 7630K

1. Introduction

In recent years, the investigation of quantum cutting downconversion by cooperative energy transfer from RE^{3+} to Yb^{3+} has been a very active field of research.[1−8] In this process, the absorption of one UV or blue photon can result in the emission of two Yb^{3+} ions around 980 nm. The quantum cutting phosphors based on cooperative energy transfer process could greatly benefit the development of Si solar cells because their emission energy is just above the band gap of Si.[9,10] If one UV–blue photon is efficiently converted into two near-infrared photons, energy loss in Si solar cells due to thermalization of electron–hole pairs will be greatly reduced. Vergeer *et al.* reported on the experimental evidence for the quantum cutting downconversion by cooperative energy transfer from one Tb^{3+} ion to two Yb^{3+} ions in the $Yb_xY_{1-x}PO_4$:Tb^{3+} powder.[1] Upon excitation of one Tb^{3+} ion with one blue photon, two near-infrared photons at 980 nm emitted from Yb^{3+} can be obtained. A similar result was reported in the RE^{3+}/Yb^{3+} (RE = Tb, Tm, Pr and Ce) codoped nanophosphors,[2−5] glasses[8] and transparent glass ceramics.[6,7]

Although the efficient cooperative energy transfer is reported in RE^{3+}/Yb^{3+} (RE = Tb, Tm, Pr) system, the infrared emission of Yb^{3+} is very weak, which is ascribed mainly to the inefficient excitation of the donors for their parity forbidden intra-configuration 4f transitions. The Ce^{3+}/Yb^{3+} system reported by Chen *et al.* overcame this shortcoming for the first time. The allowed electric-dipole transition of Ce^{3+} from the 4f ground state to the 5d excited one results in very efficient excitation. Compared with the Tb^{3+}/Yb^{3+} system, Yb^{3+} emission was reported to be enhanced greatly in Ce^{3+}/Yb^{3+} system.[8] But, Ce^{3+} has a tendency to become oxidized and Yb^{3+} has a tendency to become reduced. The luminescence quenching of a combination of this two kinds of centres from the charge transfer state RE^{4+}–RE^{2+} (Ce^{4+}–Yb^{2+}) was proposed by Blasse and Grabmaier.[11−14] This effect may reduce the real quantum efficiency greatly. Thus, it is very important to find other ions without this effect. Bi^{3+} ions have $6s^2$ electronic configuration. The $6s^2 \rightarrow 6s6p$ transition is also an allowed electric-dipole transition.[15] The emission of Bi^{3+} ions in Y_2O_3 takes place mainly around 500 nm (the energy is just twice that of the $^2F_{7/2} \rightarrow ^2F_{5/2}$ transition of Yb^{3+} ions), which suggests the possibility of efficient cooperative energy transfer from Bi^{3+} to Yb^{3+}. A similarity be-

*Project supported by the National Nature Science Foundation of China (Grant No. 10774140), the Knowledge Innovation Project of the Chinese Academy of Sciences (Grant No. KJCX2-YW-M11), the Specialized Research Fund for the Doctoral Program of Higher Education, China (Grant No. 20060358054), and the Special Foundation for Talents of Anhui Province, China (Grant No. 2007Z021).

†Corresponding author. E-mail: yinmin@ustc.edu.cn

© 2010 Chinese Physical Society and IOP Publishing Ltd

tween the ionic radii of Bi^{3+} and Y^{3+} allows for easy substitution of Bi for Y in Y_2O_3 system. It is reported that the luminescence of Eu^{3+} or Er^{3+} can be greatly intensified with the help of resonant energy transfer from the excited Bi^{3+} ions to the Eu^{3+} or Er^{3+} ones.[16,17] However, to our knowledge, there have been no reports on the efficient cooperative energy transfer from Bi^{3+} to Yb^{3+} so far. In this paper, the Bi^{3+} and Yb^{3+} codoped cubic Y_2O_3 phosphors are prepared, the efficient cooperative energy transfer from Bi^{3+} to Yb^{3+} is studied through photoluminescence characterization.

2. Experiment

Y_2O_3:Bi^{3+}, Yb^{3+} phosphors with different doping concentrations were prepared via Pechini method.[18] Y_2O_3(99.99%), $Bi(NO_3)_3{\cdot}5H_2O$ (99.99%) and Yb_2O_3 (99.99%) were used as starting materials. First, Y_2O_3, $Bi(NO_3)_3{\cdot}5H_2O$ and Yb_2O_3 were dissolved in HNO_3 (A.R.) and the solutions were mixed at a specified stoichiometric ratio. Then, citric acid was added into the mixture as complexing agent at a mole ratio of metal ions to citric acid, 1:2. Ammonia was added to adjust the pH value to about 3 at 80 °C. After strong stirring for 30 min, the solution was dried in a 80 °C water bath for 15 h. The dried gel was prefired at 450 °C in air for 1 h. Finally, products were obtained after sintering at 1000 °C for 2 h.

Powder phase was identified via x-ray diffractometry (XRD) (MAC Science Co. Ltd MXP18AHF), using nickel-filtered Cu Kα radiation in a range of $2\theta = 10^\circ - 70^\circ$, the accelerating voltage was 40.0kV and the tube current was 100.0mA. The excitation and emission spectra were obtained with a Jobin–Yvon Fluorolog 3 system. For the life-time measurements, a Q-switched frequency-tripled (355 nm) Nd:YAG laser with a pulse duration of 10 ns was used. The visible emission was dispersed by a Jobin–Yvon HRD1 double monochromator and detected by a Hamamatsu R928 photomultiplier. The near-infrared emission was dispersed by a Zolix SBP750 monochromator and detected by an Acton ID-441-C InGaAs near infrared detector. The signal was analysed by an EG&G 7265 DSP lock-in amplifier and stored into computer memories. The decay curve was measured with a Tektronix TDS2024 digital storage oscilloscope (50 Ω shunt resistance). All the measurements were carried out at room temperature.

3. Results and discussion

3.1. Structural properties

Figure 1 indicates the XRD patterns of the Y_2O_3 powder. The results show that the samples crystallized into cubic Y_2O_3 with spatial group $Ia3$ (JCPDS card No. 86-1326). The average crystallite size can be calculated by the x-ray line broadening method from the Scherrer's equation (after correction for the instrumental broadening by using a polycrystalline silicon standard): $D = 0.89\lambda/\beta\cos\theta$, where D is the crystallite size, λ is the wavelength of radiation, β is the corrected full width at half maximum and θ is the diffraction peak angle. The estimated average crystallite sizes are around 30–40 nm.

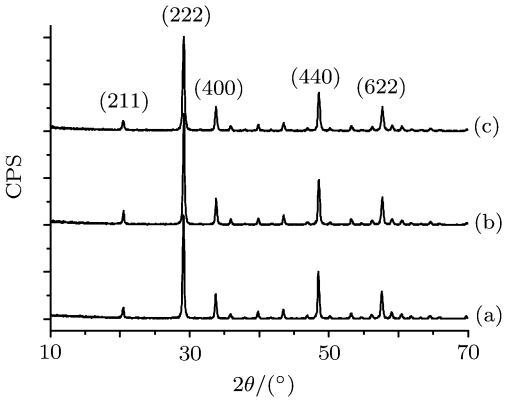


Fig. 1. XRD patterns of Y_2O_3 doped with (a) Bi0.5% (b) Bi0.5% Yb2% and (c) Bi0.5% Yb12% separately.

3.2. Photoluminescence characterization

Figure 2 shows the photoluminescence excitation (PLE) and photoluminescence (PL) spectra of the Bi^{3+} single doped Y_2O_3. The spectral results accord nicely with those of Jacobsohn.[15] In order to reduce the influence of the overlap of the emission, the PLE spectrum of the emission band centred at 491 nm was detected by monitoring the right edge (550 nm). There are an emission band with a maximum at 409 nm and a corresponding excitation band with a maximum at 370 nm, and an emission band around 491 nm corresponding to a 328 nm excitation band, separately. The Stokes shifts are 2.6×10^3 and 10.1×10^3 cm^{-1}, respectively. In cubic Y_2O_3, there are two six-coordinated non-equivalent cation sites C_2 and S_6. Their occupancies are 75% and 25%, respectively. On the basis of intensities, Boulon[19] assigned the relatively weak emission band around 409 nm to Bi^{3+} in S_6 site, and the stronger 491 nm emission band to Bi^{3+} in C_2 site. The emission energy of Bi^{3+}

in C_2 sites is just the twice that of the $^2F_{7/2} \rightarrow ^2F_{5/2}$ transition of Yb^{3+} ions, implying that the efficient cooperative energy transfer from Bi^{3+} to Yb^{3+} may take place.

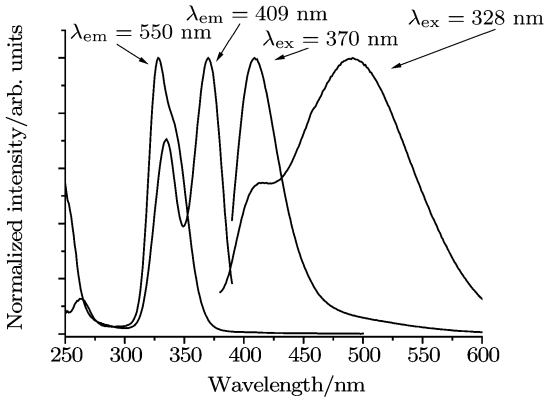


Fig. 2. PL and PLE spectra of Y_2O_3 doped with 0.5mol% Bi^{3+}.

In the excitation spectra (Fig. 3(b)) of the Bi^{3+}/Yb^{3+} codoped Y_2O_3, an excitation band ranging from 320 to 360 nm, owing to the Bi^{3+}:$6s^2$ $\rightarrow$6s6p transition, was detected by monitoring the Yb^{3+}:$^2F_{5/2} \rightarrow {}^2F_{7/2}$ emission at 979 nm, which verifies the existence of energy transfer from Bi^{3+} to Yb^{3+}. The emission spectra of the Bi^{3+}/Yb^{3+} codoped Y_2O_3 under 325 nm excitation are presented in Fig. 3(b) also. Besides the Bi^{3+} emissions in C_2 sites (491 nm) and S_6 sites (409 nm), strong Yb^{3+} emissions in a range from 950 to 1100 nm were also observed. There are mainly three emission bands at 979, 1033 and 1077 nm in this range, which is due to the stark splitting of the $^2F_{5/2} \rightarrow ^2F_{7/2}$ transition of Yb^{3+} and in good agreement with the results reported by Yuan.[2] According to Pieterson's report,[20] the charge transfer band O^{2-}–Yb^{3+} in Y_2O_3 locates in a relatively high energy region ($\lambda < 250$ nm). In the excitation spectra (Figure 3(a)) of Yb^{3+} doped Y_2O_3, there is no efficient excitation band in a range from 250 to 450 nm, which accords well with that in Pieterson's report. Thus, the observed intense UV-excited NIR emissions can only originate from the energy transfer from Bi^{3+} to Yb^{3+}. The CET of Bi^{3+}:6s6p$\rightarrow$$Yb^{3+}$:$^2F_{5/2}$+$Yb^{3+}$:$^2F_{5/2}$ is the only possible relaxation route to achieving the Yb^{3+} NIR emission because the Bi^{3+}:6s6p$\rightarrow$$6s^2$ emission is located at approximately twice the energy of the Yb^{3+}:$^2F_{7/2} \rightarrow ^2F_{5/2}$ absorption and Yb^{3+} has no other levels up to the UV region. Figure 4 shows the energy level diagrams of Bi^{3+} and Yb^{3+} ions as well as the CET process from Bi^{3+} to Yb^{3+} in the Y_2O_3 phosphors codoped with Bi^{3+} and Yb^{3+}. In this system, a Bi^{3+} ion absorbs a UV photon and is excited from the ground state ($6s^2$) to the excited state (6s6p). The excited sate will relax to the ground state by emitting a blue–green photon or through CET to two nearby Yb^{3+} ions accompanied by the emission of two NIR photons. The strong stokes shift between the absorption and the emission of the Bi^{3+} ion is ascribed to the vibration relaxation of the host.

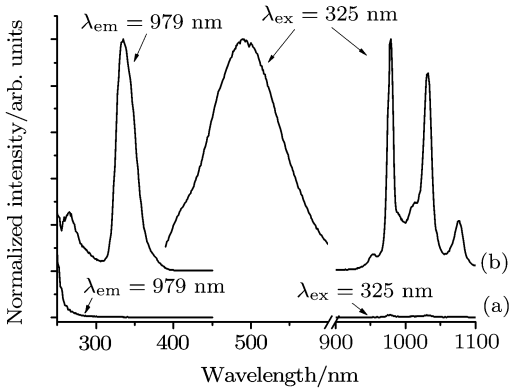


Fig. 3. PL and PLE spectra of (a) Y_2O_3 doped with 1 mol% Yb^{3+} and (b) Y_2O_3 codoped with 0.5 mol% Bi^{3+} and 1 mol% Yb^{3+}.

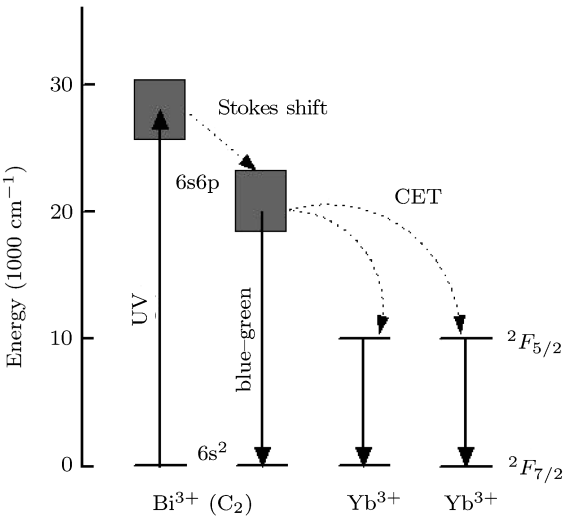


Fig. 4. Schematic energy level diagrams of Bi^{3+} and Yb^{3+} in Y_2O_3 and the CET mechanism for the NIR QC emission under UV excitation.

The dependences of the Bi^{3+} and Yb^{3+} emission intensities on Yb^{3+} doping concentration of the Y_2O_3 phosphors codoped with 0.5 mol% Bi^{3+} and x mol% Yb^{3+} upon excitation at 325 nm are shown in Fig. 5. It is noticed that the PL intensity of the NIR emission at 979nm increases rapidly with the increase of Yb^{3+} concentration ranging from 0 to 2 mol%, while emission of Bi^{3+} ions at 500 nm decreases monotonically.

However, at higher Yb^{3+} concentrations, cross relaxation takes place between Yb^{3+} ions, which effectively reduces luminescence yield. A decrease of the NIR emission at 979 nm has been clearly observed when Yb^{3+} concentration is set to be more than 2 mol%, due to concentration quenching. The decay curves of Yb^{3+} upon excitation of Bi^{3+} are shown in the inset of Fig. 5. The life-time decreases monotonically from 880 to 126 μs with Yb^{3+} concentration increasing from 1 mol% to 12mol%, which further verifies Yb^{3+} concentration quenching.

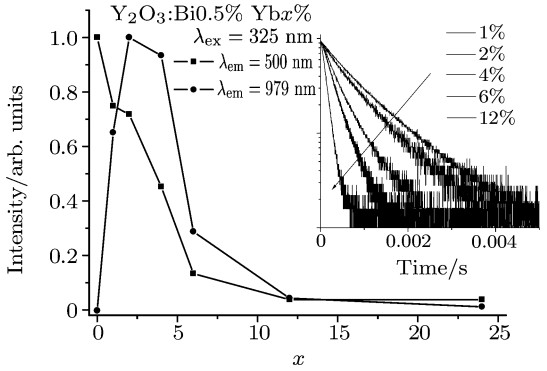


Fig. 5. Dependences of the Bi^{3+} and Yb^{3+} emission intensities on the Yb^{3+} doping concentration in Y_2O_3:Bi^{3+}0.5%, Yb^{3+} phosphors. Inset shows the decay curves of the Yb^{3+}:$^2F_{5/2} \rightarrow {}^2F_{7/2}$ luminescence at 979 nm for samples with various Yb^{3+} contents.

Figure 6 shows the luminescence decay curves of Bi^{3+} emission intensity for Y_2O_3 doped with 0.5 mol% Bi^{3+} and 0–24 mol% Yb^{3+} upon excitation at 355 nm. The decay curves of a singly doped Y_2O_3:Bi0.5% phosphor fit well to a single exponential function with a decay life-time of 733 ns. However, the decay life-time decreases rapidly from 733 to 309 ns with Yb^{3+} doping concentration increasing from 0 mol% to 24 mol%. The faster decline in the life-time as a function of Yb^{3+} concentration can be explained by the introduction of extra decay pathways due to the Yb^{3+} doping: ET from Bi^{3+} to Yb^{3+} which enhances the Bi^{3+} decay rate. These results give a further evidence of the efficient CET from Bi^{3+} to Yb^{3+}. From the luminescence decay curves, the CET efficiency ($\eta_{\rm CET}$) and the total theoretical downconversion quantum efficiency ($\eta_{\rm QE}$) could be estimated from the following equations:[1–8]

$$\eta_{{\rm CET},x\%{\rm Yb}} = 1 - \frac{\int I_{x\%{\rm Yb}}{\rm d}t}{\int I_{0\%{\rm Yb}}{\rm d}t},$$

$$\eta_{\rm QE} = \eta_{\rm Bi}\,(1 - \eta_{\rm CET}) + 2\eta_{\rm Yb}\eta_{\rm CET},$$

where I denotes the decay intensity, x%Yb represents the Yb^{3+} content, $\eta_{\rm Bi}$ and $\eta_{\rm Yb}$ refer to the luminescence quantum efficiencies of Bi^{3+} and Yb^{3+}, respectively. With Yb^{3+} content increasing from 1 to 24 mol%, the CET efficiency increases monotonically from 5.4% to 39.5% as shown in the inset of Fig. 6. By ignoring the quench process and setting the quantum efficiencies of Bi^{3+} and Yb^{3+} ($\eta_{\rm Bi}$ and $\eta_{\rm Yb}$) as 1, the upper limited values of the theoretical quantum efficiency are calculated to be 105.4%, 105.9%, 115.6%, 124.4%, 137%, 139.5% for samples with the Yb^{3+} doping concentrations equal to 1%, 2%, 4%, 6%, 12% and 24%, respectively.

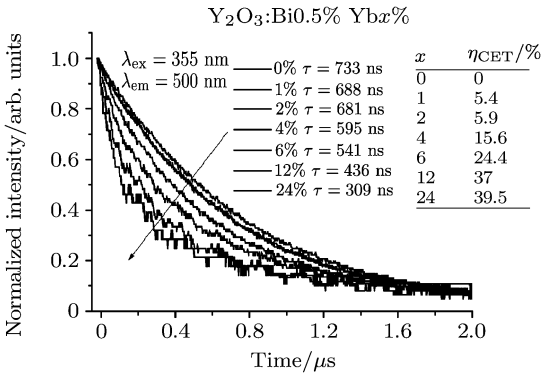


Fig. 6. Decay curves of the Bi^{3+}:6s6p$\rightarrow$6s^2 luminescence at 500 nm for samples with various Yb^{3+} contents. The inset shows the CET efficiency ($\eta_{\rm CET}$) as a function of Yb^{3+} contents.

It should be noted that the concentration quenching of Yb^{3+} emission is a serious problem for the application of this quantum cutting downconversion material. If we use the equation which is used to calculate the CET efficiency ($\eta_{\rm CET}$), the efficiency of the energy transfer from the Yb^{3+} to quenching centres can be obtained from the luminescence decay cures of Yb^{3+} (the sample with Yb^{3+} 1 mol% is deemed to have no energy transfer from the Yb^{3+} to the quenching centres and used as the standard). The efficiencies are 17.6%, 47.7%, 66.3% and 81.1% for samples with the Yb^{3+} doping concentrations equal to 2%, 4%, 6% and 12%, respectively. So, the quantum efficiency of Yb^{3+} ($\eta_{\rm Yb}$) is far from 1 (only 18.9% for the sample with Yb^{3+} 12%) because of the concentration quenching effect. Overcoming the concentration quenching effect of Yb^{3+} and increasing the practical QC efficiency are a most challenge task in further research.

4. Conclusion

The downconversion phosphors of Bi^{3+}/Yb^{3+} codoped Y_2O_3 are prepared and studied by photo-

luminescence excitation spectra and time-resolved luminescence techniques. It is demonstrated that Bi^{3+} ion can efficiently transfer their energy to two neighbouring Yb^{3+} ions by the CET process. The results indicate that this material has a potential application in the high efficiency silicon-based solar cells by down-conversion of one UV photon which is almost useless in the silicon solar cell to two NIR photons around 980 nm where the Si solar Cell exhibits the greatest spectral response.

References

[1] Vergeer P, Vlugt T J H, Kox M H F, den Hertog M I, van der Eerden J P J M and Meijerink A 2005 *Phys. Rev.* B **71** 014119

[2] Yuan J L, Zeng X Y, Zhao J T, Zhang Z J, Chen H H and Yang X X 2008 *J. Phys.* D: *Appl. Phys.* **41** 105406

[3] Zhang Q Y, Yang C H and Jiang Z H 2007 *Appl. Phys. Lett.* **90** 061914

[4] Zhang Q Y and Yang C H 2007 *Appl. Phys. Lett.* **90** 021107

[5] Xie L C, Wang Y H and Zhang H J 2009 *Appl. Phys. Lett.* **94** 061905

[6] Ye S, Zhu B, Chen J X, Luo J and Qiu J R 2008 *Appl. Phys. Lett.* **92** 141112

[7] Chen D Q, Wang Y S, Yu Y L, Huang P and Weng F Y 2008 *Opt. Lett.* **33** 1884

[8] Chen D Q, Wang Y S, Yu Y L, Huang P and Weng F Y 2008 *J. Appl. Phys.* **104** 116105

[9] Richards B S 2006 *Sol. Energy Mater. Sol. Cells* **90** 2329

[10] Jin X, Zhang X D, Lei Z F, Xiong S Z, Song F and Zhao Y 2008 *Acta Phys. Sin.* **57** 4580 (in Chinese)

[11] Blasse G and Grabmaier B C 1994 *Luminescent Materials* (Berlin: Springer)

[12] Verweij J W M, Pedrini C, Bouttet D, Dujardin C, Lautesse H and Moine B 1995 *Opt. Mater.* **4** 575

[13] Rivas-Silva J F, Durand-Niconoff S, Schmidt T M and Berrondo M 2000 *Int. J. Quantum Chem.* **79** 198

[14] Vergeer P, Babin V and Meijerink A 2005 *J. Lumin.* **114** 267

[15] Jacobsohn L G, Blair M W, Tornga S C, Brown L O, Bennett B L and Muenchausen R E 2008 *J. Appl. Phys.* **104** 124303

[16] Chi L S, Liu R S and Lee B J 2005 *J. Electrochem. Society* **152** 8

[17] Xu Q H, Lin B C and Mao Y L 2005 *J. Lumin.* **128** 1965

[18] Huang P, Cui C and Wang S 2009 *Chin. Phys.* B **18** 4524

[19] Boulon G 1971 *J. Phys.* (Paris) **32** 333

[20] van Pieterson L, Heeroma M, de Heer E and Meijerink A 2000 *J. Lumin.* **91** 177